

The importance of Icelandic ice sheet growth and retreat on mantle CO₂ flux

John J. Armitage¹, David J. Ferguson², Kenni D. Petersen³, and Timothy T. Creyts⁴

¹Dynamique des Fluides Géologiques, Institut de Physique du Globe de Paris, Paris, France

²School of Earth and Environment, University of Leeds, Leeds, U.K.

³Department of Geoscience, University of Aarhus, Aarhus, Denmark

⁴Lamont-Doherty Earth Observatory, Columbia University, U.S.A

Key Points:

- We combine a new history of Icelandic ice-cover with a forward model of magma generation.
- Peak mantle CO₂ flux is non-linearly related to magmatic eruption rates.
- Icelandic CO₂ degassing likely peaked first at 60 ka, and secondly with three pulses between 20 and 10 ka.

15 **Abstract**

16 Climate cycles may significantly affect the eruptive behavior of terrestrial volcanoes due
 17 to pressure changes caused by glacial loading, which raises the possibility that climate
 18 change may modulate CO₂ degassing via volcanism. In Iceland, magmatism is likely to
 19 have been influenced by glacial activity. To explore if deglaciation therefore impacted
 20 CO₂ flux we coupled a model of glacial loading over the last ~120 ka to melt generation
 21 and transport. We find that a nuanced relationship exists between magmatism and glacial
 22 activity. Enhanced CO₂ degassing happened prior to the main phase of late-Pleistocene
 23 deglaciation, and it is sensitive to the duration of the growth of the ice sheet entering
 24 into the LGM, as well as the rate of ice loss. Ice sheet growth depresses melting in the
 25 upper mantle, creating a delayed pulse of CO₂ out-gassing as the magmatic system re-
 26 covers from the effects of loading.

27 **1 Introduction**

28 Evidence from several tectonic settings indicates that glaciated volcanic systems
 29 respond to changing ice volumes (Glazner, Manley, Marron, & Rojstaczer, 1999; Jellinek,
 30 Mange, & Saar, 2004; Jull & McKenzie, 1996; MacLennan, Jull, McKenzie, Slater, & Grönvöld,
 31 2002; Rawson et al., 2016; Sigvaldsson, Annertz, & Nilsson, 1992), and suggests there was
 32 a widespread volcanic response to late-Pleistocene ice retreat (Huybers & Langmuir, 2009).
 33 The most compelling evidence for climate-coupled volcanism comes from Iceland, where
 34 changes in early Holocene lava volumes and magma chemistry are consistent with de-
 35 pressurization during glacial unloading (Jull & McKenzie, 1996; MacLennan et al., 2002;
 36 Sinton, Grönvöld, & Saemundsson, 2005). Magma generation here occurs due to pressure-
 37 release melting, as the mantle up-wells beneath rift zones. Although the net change in
 38 overburden pressures from variations in ice cover have been relatively small, the high rates
 39 of change associated with glacial activity can produce significant short-term fluctuations
 40 in magmatic output (Jull & McKenzie, 1996; Pagli & Sigmundsson, 2008; Schmidt et al.,
 41 2013). Carbon readily partitions into magmas during partial melting (Rosenthal, Hauri,
 42 & Hirschmann, 2015) and is released as a CO₂ rich fluid/vapour as the magma ascends
 43 through the crust, making volcanism the primary pathway for transporting carbon from
 44 the Earth's mantle to the atmosphere (Dasgupta & Hirschmann, 2010). However, car-
 45 bon does not enter the melt uniformly during partial melting and is concentrated in early
 46 formed magma. Therefore the extent to which glacially driven changes in primary magma
 47 generation alter the flux of CO₂ depends on where in the melting column melt produc-
 48 tion is enhanced (or suppressed), the rate of melt transport, and the history of ice sheet
 49 growth and retreat.

50 It is thought that CO₂ and the trace element Nb have a relatively similar behaviour
 51 during decompression melting (Saal, Hauri, Langmuir, & Perfit, 2002), and as such Nb
 52 compositions can be used to gauge the quantity of CO₂ erupted. In Iceland there are just
 53 over 300 published dated analysis of the Nb composition of Pleistocene lavas (Eason, Sin-
 54 ton, Grönvöld, & Kurz, 2015; Gee, Taylor, Thirwall, & Murton, 1998). This is arguably
 55 the most complete geochemical record of Nb compositions within a region that experi-
 56 enced significant Pleistocene deglaciation. In this study we take a new approach, and
 57 use a high resolution model of ice sheet history to drive a forward model of melt gen-
 58 eration and transport, and predict CO₂ degassing. We validate the model predictions
 59 against the seismic structure imaged below Iceland, and the observed crustal thickness.
 60 We subsequently explore under what conditions climate and magmatism might be re-
 61 lated, and the implications for CO₂ degassing.

62 **2 Methods**

63 **2.1 Modelling of Melt Generation and Transport**

64 We develop a model of magma generation and transport coupled to a model of the
 65 flexure of a viscoelastic beam for the response to change in load due to the ice sheet his-
 66 tory (see Supplementary Material). The coupled model consists of a flexural model of
 67 the surface displacement due to the changing surface load as the ice sheet changes in thick-
 68 ness. This model of surface displacement is then coupled to either a 1D vertical column,
 69 or a 2D corner flow model where the flow of the mantle is prescribed at either an up-
 70 welling rate of 10 or 20 mm yr⁻¹, or lateral spreading rate of 10 mm yr⁻¹. We use these
 71 two upwelling rates to cover the uncertainty in the exact rate of vertical ascent the man-
 72 tle below Iceland due to mantle buoyancy. The upwelling column is perturbed by the
 73 displacement due to loading, where the viscoelastic decay time of the load is set to 1000 yrs.
 74 The upper surface of the melting model is held at 30 km to be consistent with the Moho
 75 depth, which is in the range of 20 to 40 km below Iceland (Jenkins et al., 2018). Carbon
 76 partitioning into the melt is assumed to be governed by the coefficients derived by Rosen-
 77 thal et al. (2015). We use a mantle source composition for Nb of 1.627 ppm, which is in-
 78 termediate between the end-member sources for Icelandic melts identified by (Shorttle
 79 & MacLennan, 2011). To approximate the melting of the multiple source lithologies we
 80 chose a solidus-depletion gradient of 600 °C which is intermediate between that of melt-
 81 ing experiments on depleted mantle, 900 °C (Wasylenki, Baker, Kent, & Stopler, 2003)
 82 and fertile mantle 300 °C (Scott, 1992).

83 To constrain permeability, we examined the effects of varying the permeability co-
 84 efficient on the seismic properties of the mantle produced by our 1-D model. The ther-
 85 mal structure and porosity was converted to S-wave velocities, assuming that melt re-
 86 duces the velocity by 7.9 % per percent porosity (Hammond & Humphreys, 2000) and
 87 including the effects of attenuation (Goes, Armitage, Harmon, Huismans, & Smith, 2012).
 88 Recent joint inversion of teleseismic and ambient noise Rayleigh waves in Iceland would
 89 suggest that the S-wave velocity is between 4 and 3.8 km s⁻¹ at depths of 50 to 150 km
 90 (Harmon & Rychert, 2016) (Figure 1). We find that the permeability coefficient, k_0 , needs
 91 to be relatively high (10^{-5} m²) giving a permeability, $k_\phi = k_0\phi^3$ (where ϕ is porosity),
 92 of the order of 10^{-14} m² ($\phi \approx 0.001$; Figure 1), because otherwise porosity would be
 93 too large and the S-wave velocity would decrease below the observed values. This per-
 94 meability is an order of magnitude higher than the upper range used to explore how sea-
 95 level change might influence mid-ocean ridge (MOR) magmatism (Burley & Katz, 2015;
 96 Crowley, Katz, Huybers, Langmuir, & Park, 2015), and suggests rates of magmatic as-
 97 cent of the order of 10 m yr⁻¹, in agreement with MacLennan et al. (2002). Previously
 98 it has been suggested that delays in signal propagation from the zone of partial melt-
 99 ing at MORs to the surface might be of the order of a Milankovitch-scale period, 40 kyr
 100 (Huybers & Langmuir, 2017). However, the high permeability required to match the seis-
 101 mic observations from Iceland implies a magmatic system that much more rapidly re-
 102 sponds to change in melting conditions, consistent with the fast transport rates estimated
 103 from U-series isotope studies (Elliot & Spiegelman, 2014).

104 **2.2 Glacial Forcing Throughout the Pleistocene**

105 Iceland experienced extensive ice-cover during the last glacial period (Patton, Hub-
 106 bard, Bradwell, & Schomackere, 2017), with maximum thicknesses in the center of the
 107 island of ~ 2 km attained by ~ 23 ka (Figure 2a and b). Deglaciation after the LGM oc-
 108 curred at a varying rate, and was discontinuous. For example, a stage of re-advance oc-
 109 curred during the colder climate of the Younger Dryas (11.7-12.9 ka) (Nordahl & Ingólfsson,
 110 2015). The final phase of deglaciation was particularly rapid, with the main volcanic zones
 111 being largely ice free by ~ 10 ka (Figure 2a). The most uncertain period of the glacial
 112 history is the pre-LGM growth of the ice sheet. To create the ice sheet histories shown

in Figure 2b and Figure 3a we calibrated the ice volume since the LGM against the North Greenland Ice Core Project (NGRIP) $\delta^{18}\text{O}$ record, and Quaternary sea-level curves assuming a linear correlation between these three signals (see Supplementary Material Text S1). We focus on two scenarios: M1, based on the ICE-5G sea-level curves (Peltier, 2004), and M2, based on the sea-level curves of Pico, Creveling, and Mitrovica (2017) (Figure S2).

3 Results

3.1 Effect of glacial loading and unloading

We force our melt model with the 120 ka glacial history after a 5 Myr model wind-up to steady state (model M1, Figure 2b) and using a single value for the ice thickness at each time-step, therefore neglecting the effects of the distal parts of the ice sheet on melting beneath the rift margins. The impact of deglaciation events is modulated by the upwelling rate of the solid mantle because the upwelling rate controls the background productivity of the melting model. At slower upwelling rates, i.e. 10 mm yr^{-1} , some periods of deglaciation are not recorded in the flux of magma erupted. An example of this is the warming event at 60 ka (Figure 2), where the 10 mm yr^{-1} upwelling model produces no response in either the eruption rate or CO_2 flux. If however upwelling is more rapid, 20 mm yr^{-1} , then there is a clear pulse in melt eruption rate (Figure 2). For a more productive scenario, there is increased shallow melting. The displacement imposed by the flexural response to unloading dissipates with depth. Therefore, if melting is productive and hence shallow it will feel the effects of the unloading to a greater extent when compared to a less productive melting system. Furthermore, when productivity is low, the porosity is low and the rate of vertical melt flow is slow such that a pulse in melt production will not reach the surface rapidly.

The magnitude of CO_2 flux peaks are not linearly related to the magnitude in eruption rates (Figure 2d). For example, in the 20 mm yr^{-1} upwelling rate model, the largest CO_2 peak is estimated to occur at ~ 60 ka and not during the volumetrically larger magmatic pulse at the end of the Pleistocene (Figure 2d). This difference is because when the ~ 60 ka warming occurred, the melt was enriched in carbon due to the preceding rapid glaciation. Magma supplied from the mantle during the Late-Pleistocene pulse were more depleted in carbon compared to those in the 60 ka event. The implication of this result is that volumetrically small volcanic events might have just as a strong influence on CO_2 degassing as the more significant periods of volcanic eruptions, and the magnitude of CO_2 degassing is dependent on the history of glacial forcing.

3.2 Glacial Forcing Through the Latest Pleistocene and Holocene

During the last 40 ka, our model suggest that CO_2 flux is highly dependent on the glacial forcing. There are two distinct late Pleistocene magmatic pulses, separated by the Younger Dryas cold period (Figure 3a and b). However, for the model M2 ice sheet history there are three pulses in CO_2 flux at the end of the Pleistocene, due to the faster ice sheet growth entering the LGM from 35 to 25 ka in this model (Figure 3a and e). This peak in CO_2 flux is because the small magnitude but rapid deglaciations after 25 ka tap melts rich in trace elements including Nb and carbon (Figure 3c and d).

The observed time series of incompatible trace element concentrations in Icelandic magmas and ice sheet history have been suggested to be strongly associated (Eason et al., 2015; Gee et al., 1998; Jull & McKenzie, 1996; MacLennan et al., 2002; Sinton et al., 2005). Of these studies Gee et al. (1998) and Eason et al. (2015) report on the Nb composition of lavas erupted and give age ranges for the erupted lavas. Dating lava flow in Iceland is complex given the lack of reliable markers from which ages can be obtained. This means that ages are instead typically taken from the morphology and tephrochronol-

162 ogy of erupted flows (MacLennan et al., 2002), which is subjective and open to debate.
 163 We therefore take the age ranges for the Nb compositions reported by Gee et al. (1998),
 164 Sinton et al. (2005), and Eason et al. (2015) as indicative, and so chose to bin the ages
 165 into 2.5 kyr intervals from 0 to 17.5 ka and then at 5 kyr intervals (Figure 3c). The re-
 166 duction in Nb compositions plotted is in line with the trends observed within the more
 167 selective La and Sm data set presented in MacLennan et al. (2002), and is therefore likely
 168 robust.

169 We find that the predicted change in Nb from all our models fits within the range
 170 of the observations (Figure 3c). The M2 model gives the strongest signature in Nb con-
 171 centrations of deglaciation during the end of the Pleistocene, while the signature is more
 172 subdued in the M1 ice sheet model (Figure 3c). The 1D forward model used is highly
 173 idealised, and yet the agreement between the observations and model is encouraging, and
 174 suggests the compositional change observed in lavas erupted during the late-Pleistocene
 175 to early Holocene is due to rapid deglaciation (Eason et al., 2015; Gee et al., 1998; Maclen-
 176 nan et al., 2002; Sinton et al., 2005). This implies that the observed change in melt com-
 177 position is due to change in ice sheet loading and that the pre-deglaciation volcanism
 178 likely released a significant volume of CO₂ (Figure 3e).

179 The 1D column model will underestimate the impact of change in deep melt pro-
 180 ductivity, as it cannot capture the deep wings of the zone of partial melting. To explore
 181 the impact of this we force a series of 1D models with the vertical flow taken from steady
 182 state corner flow perturbed by the flexural response of the deglaciation of a 200 km wide
 183 ice sheet. The half spreading rate is assumed to be 10 mm yr⁻¹, and the mantle poten-
 184 tial temperature is 1450 °C. Melt travels vertically from the zone of partial melting in
 185 columns at 0 to 80 km from the rift axis (Figure 4). The steady state thickness of melt
 186 erupted at the surface of the simplified 2D model is 20 km (Figure S4), and glacial forc-
 187 ing causes this thickness to vary around this value by the order of 10 km except for a large
 188 spike at the LGM. The crust of Iceland varies in thickness from 20 to 40 km (e.g. Jenk-
 189 ins et al., 2018), and therefore a model steady state thickness of 20 km is a reasonable
 190 lower end-member prediction given that the crust is made of both extrusions and intru-
 191 sions.

192 After glacial perturbation we find that in the central zone, from the ridge centre
 193 to 40 km distance, the trend in Nb and CO₂ flux is relatively similar, with a reduction
 194 in Nb at 15 ka. At distances greater than 40 km, a peak in Nb and CO₂ flux is predicted
 195 to occur with an increasing delay compared to the centre of extension (Figure 4). This
 196 delay is due to the greater distance that the melt has to travel along the vertical path
 197 from the top of the melt zone to the surface at increasing distance from the centre of ex-
 198 tension. In full 2D models the distal melt will pool as it migrates laterally towards the
 199 centre of extension (Katz, 2008), yet the difference in ascent velocity due to the increase
 200 porosity as the melt pools would likely not be sufficient to overcome the increased dis-
 201 tance that the signal will have to travel.

202 The full solution to the coupled equations of magma dynamics would suggest that
 203 melts generated at a distance of up to 60 km from the centre of extension are advected
 204 to the ridge axis (Katz, 2008). If all of the melt generated up to 60 km from the centre
 205 of extension is erupted, then the CO₂ flux is significantly increased during the Holocene
 206 due to the addition input of melt from the distal parts of the zone of partial melting (Fig-
 207 ure 4b). Therefore these low productivity and deep regions of the zone of partial melt-
 208 ing might be a key exporter of mantle carbon into the atmosphere. However, the range
 209 of observed Nb concentrations are relatively similar to the axial concentrations, from within
 210 <40 km of the rift centre (Figure 4). This would suggest that the widest regions of the
 211 zone of partial melting are not sampled by the volcanism in the Reykjanes Ridge and
 212 Western Volcanic Zone, leading to an estimate of CO₂ fluxes more in line with the sim-
 213 pler 1D model.

214 4 Discussion and Conclusions

215 The models imply that the deglaciation beginning at 18 ka and continuing through
 216 the Bölling warming at 14.8 ka released substantial quantities of CO₂ when compared
 217 to the last 120 ka (Figure 3c and Figure 4b), and this elevated CO₂ release was because
 218 of the preceding growth of the ice sheet. Volcanism during this time would have taken
 219 place in a sub-glacial environment and unsurprisingly does not feature in the post-glacial
 220 sub-aerial record. Evidence from sub-glacial volcanic units (tuyas) erupted during this
 221 time period (Hartley, Thordarson, & de Joux, 2016) suggest volumetric and composi-
 222 tional trends consistent with those predicted by our model (Figure 3c and Figure 4).

223 Forcing our model with the long-term 120 ka ice sheet history produces a periodic
 224 fluxing of CO₂ from Icelandic volcanoes due to ice-loss events over this period, implying
 225 a close link between ice dynamics and magmatic out-gassing. The greatest release
 226 of CO₂, however, occurred during the period of ice-loss just before the Younger Dryas
 227 (\sim 14 ka), and therefore before the largest phase of late-Pleistocene deglaciation (Figure
 228 4). The concentration of CO₂ released in this magmatic pulse was enhanced due to the
 229 lack of any significant loss of ice volume since \sim 40 ka. This created a magmatic system
 230 capable of fluxing large volumes of carbon during the initial period of post-LGM deglacia-
 231 tion (both models M1 and M2, Figure 3e), possibly contributing to the increased atmo-
 232 pheric CO₂ levels thought to be recorded between 15 and 14 ka in the EPICA Dome C
 233 ice core (Köhler, Knorr, Buiiron, Lourantou, & Chappellaz, 2011). It is therefore possi-
 234 ble that this pulse of magmagenic CO₂, from Iceland and elsewhere (e.g. /citephuybers-
 235 2009, bolstered the climate warming, and final phase of deglaciation, that proceeded the
 236 Younger Dryas.

237 The CO₂ flux due to deglaciation is strongly influenced by the ice sheet history.
 238 Mantle CO₂ flux does not follow a linear relationship with eruption rates: large peaks
 239 in CO₂ are also predicted for periods in time when the volume flux is not very high (Fig-
 240 ure 2d and 3e). In effect we cannot conclude that all deglaciation events, or other rapid
 241 unloading events due to for example erosion (e.g. Sternai, Caricchi, Castelltort, & Cham-
 242 pagnac, 2016), lead to a large flux of volatile gases into the Earths atmosphere.

243 Supporting Information

244 A detailed discussion of the methodology can be found in the supporting informa-
 245 tion (Andersen et al., 2004; Andrews, 2008; Armitage, Collier, Minshull, & Henstock, 2011;
 246 Clark et al., 2009; Geirsdóttir, 2011; Gibson & Geist, 2010; Gurendo & Chaussidon, 1995;
 247 Katz, Spiegelman, & Langmuir, 2003; Lambeck & Chappel, 2001; Lambeck, Rouby, Pur-
 248 cell, Sun, & Sambridge, 2014; McKenzie & O’Nions, 1991; Miller, Zhu, Montési, & Gae-
 249 tani, 2014; Ribe, 1985; Scott, 1992; Shorttle & Macleman, 2011; Silbeck, 1975; Sleep &
 250 Snell, 1976; Spiegelman, 1996; Spratt & Lisicki, 2016).

251 Acknowledgments

252 We would like to thank M. A. Mary Gee (The University of Western Australia) for shar-
 253 ing her Nb composition data from the Reykjanes Peninsula, and Tamara Pico (Harvard
 254 University) for sharing her sea level curves. John J. Armitage acknowledges funding from
 255 an Agence Nationale de la Recherche (France), Accueil de Chercheurs de Haute Niveau,
 256 grant InterRift. Numerical computations were partly performed on the S-CAPAD plat-
 257 form, IPGP, France. The 1-D melting model is available from <https://bitbucket.com/johnjarmitage/melt1d-icesheet/>

259 References

260 Andersen, K. K., Azuma, N., Barnola, J. M., Bigler, M., Biscaye, P., Caillon, N.,

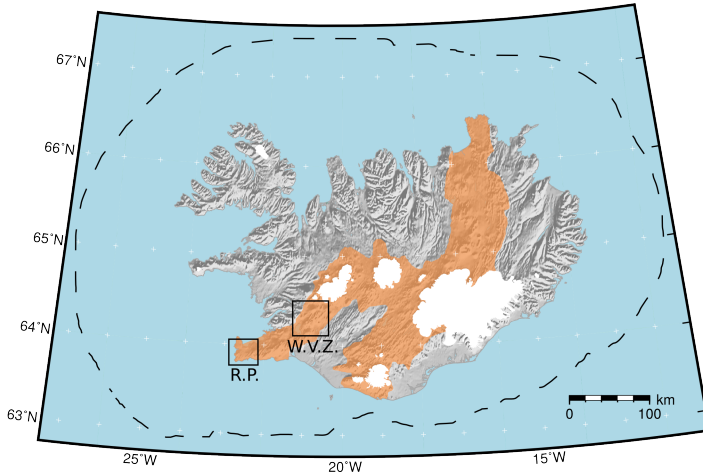
- 261 ... White, J. W. C. (2004). High-resolution record of northern hemisphere
 262 climate extending into the last interglacial period. *Nature*, *431*, 174-151. (doi:
 263 10.1038/nature02805)
- 264 Andrews, J. T. (2008). The role of the Iceland Ice Sheet in the North Atlantic dur-
 265 ing the late Quaternary: a review and evidence from Denmark Strait. *Journal*
 266 *of Quaternary Science*, *23*, 3-20. (doi: 10.1002/jqs.1142)
- 267 Armitage, J. J., Collier, J. S., Minshull, T. A., & Henstock, T. J. (2011). Thin
 268 oceanic crust and flood basalts: India-Seychelles breakup. *Geochemistry Geo-*
 269 *physics Geosystems*, *12*(Q0AB07). (doi:10.1029/2010GC003316)
- 270 Burley, J. M. A., & Katz, R. F. (2015). Variations in mid-ocean ridge CO₂ emis-
 271 sions driven by glacial cycles. *Earth and Planetary Science Letters*, *426*, 246-
 272 258. (doi: 10.1016/j.epsl.2015.06.031)
- 273 Clark, P. U., Dyle, A. S., Shakun, J. D., Carlson, A. E., Clark, J., Wohlfarth, B., ...
 274 McCabe, A. M. (2009). The last glacial maximum. *Science*, *325*, 710. (doi:
 275 10.1126/science.1172873)
- 276 Crowley, J. W., Katz, R. F., Huybers, P., Langmuir, C. H., & Park, S. H. (2015).
 277 Glacial cycles drive variations in the production of oceanic crust. *Science*, *347*,
 278 1237-1240. (doi: 10.1126/science.1261508)
- 279 Dasgupta, R., & Hirschmann, M. M. (2010). The deep carbon cycle and melting
 280 in Earth's interior. *Earth and Planetary Science Letters*, *298*, 1-13. (doi:
 281 10.1016/j.epsl.2010.06.039)
- 282 Eason, D. E., Sinton, J. M., Gronvöld, K., & Kurz, M. D. (2015). Effects of
 283 deglaciation on the petrology and eruptive history of the Western Volcanic
 284 Zone, Iceland. *Bulletin of Volcanology*, *77*(47). (doi: 10.1007/s00445-015-0916-
 285 0)
- 286 Elliot, T., & Spiegelman, M. (2014). Melt migration in oceanic crustal production:
 287 A u-series perspective. In *Treatise on geochemistry* (2nd ed., p. 543-581). Else-
 288 vier. (doi: 10.1016/B978-0-08-095975-7.00317-X)
- 289 Gee, M. A. M., Taylor, R. N., Thirwall, M., & Murton, B. J. (1998). Glacioisostacy
 290 controls chemical and isotopic characteristics of tholeiites from the Reykjanes
 291 Peninsula, SW Iceland. *Earth and Planetary Science Letters*, *164*, 1-5.
- 292 Geirsdóttir, A. (2011). Pliocene and pleistocene glaciations of iceland: a brief
 293 overview of the glacial history. In J. Ehlers, P. L. Gibbard, & P. Hughes
 294 (Eds.), *Quaternary glaciations - extent and chronology, a closer look* (Vol. 15,
 295 p. 199-210). Elsevier. (doi: 10.1016/B978-0-444-53447-7.00016-7)
- 296 Gibson, S. A., & Geist, D. (2010). Geochemical and geophysical estimates of litho-
 297 spheric thickness variation beneath galápagos. *Earth and Planetary Science*
 298 *Letters*, *300*, 275-286. (doi: 10.1016/j.epsl.2010.10.002)
- 299 Glazner, A. F., Manley, C. R., Marron, J. S., & Rojstaczer, S. (1999). Fire
 300 or ice: Anticorrelation of volcanism and glaciation in california over the
 301 past 800,000 years. *Geophysical Resaerch Letters*, *26*, 1759-1762. (doi:
 302 10.1029/1999GL900333)
- 303 Goes, S., Armitage, J. J., Harmon, N., Huismans, R., & Smith, H. (2012). Low seis-
 304 mic velocities below mid-ocean ridges: Attenuation vs. melt retention. *Journal*
 305 *of Geophysical Research*, *117*, B12403. (doi: 10.1029/2012JB009637)
- 306 Gurenko, A. A., & Chaussidon, M. (1995). Enriched and depleted primitive melts
 307 included in olivine from icelandic tholeiites: Origin by continuous melting of a
 308 single mantle column. *Geochimica et Cosmochimica Acta*, *59*, 2905-2917.
- 309 Hammond, W. C., & Humphreys, E. D. (2000). Upper mantle seismic wave ve-
 310 locity: Effects of realistic partial melt geometries. *Journal of Geophysical Re-*
 311 *search*, *105*, 10975-10986.
- 312 Harmon, N., & Rychert, C. A. (2016). Joint inversion of teleseismic and ambient
 313 noise Rayleigh waves for phase velocity maps, an application to Iceland. *Jour-*
 314 *nal of Geophysical Research*, *121*, 5966-5987. (doi: 10.1002/2016JB012934)
- 315 Hartley, M. E., Thordarson, T., & de Joux, A. (2016). Postglacial eruptive history

- of the Askja region, North Iceland. *Bulleting of Volcanology*, 78(28). (doi: 10.1007/s00445-016-1022-7)
- Huybers, P., & Langmuir, C. H. (2009). Feedback between deglacation, volcanism, and atmospheric CO₂. *Earth and Planetary Science Letters*, 286, 479-491. (doi: 10.1016/j.epsl.2009.07.014)
- Huybers, P., & Langmuir, C. H. (2017). Delayed CO₂ emissions from mid-ocean ridge volcanism as a possible cause of late-Pleistocene glacial cycles. *Earth and Planetary Science Letters*, 457, 238-249. (doi: 10.1016/j.epsl.2016.09.021)
- Jellinek, M. A., Mange, M., & Saar, M. O. (2004). Did melting glaciers cause volcanic eruptions in eastern California? probing the mechanisms of dike formation. *Journal of Geophysical Research*, 109(B09206). (doi: 10.1029/2004JB002978)
- Jenkins, J., MacLennan, J., Green, R. G., Cottaar, S., Deuss, A. F., & White, R. S. (2018). Crustal formation on a spreading ridge above a mantle plume: Receiver function imaging of the Icelandic crust. *Journal of Geophysical Research*, 123, 5190-5208. (doi: 10.1029/2017JB015121)
- Jull, M., & McKenzie, D. (1996). The effect of deglaciation on mantle melting beneath Iceland. *Journal of Geophysical Research*, 101(B10), 21815-21828.
- Katz, R. F. (2008). Magma dynamics with the enthalpy method: Benchmark solutions and magmatic focusing at mid-ocean ridges. *Journal of Petrology*, 49, 2099-2121. (doi:10.1093/petrology/egn058)
- Katz, R. F., Spiegelman, M., & Langmuir, C. H. (2003). A new parameterization of hydrous mantle melting. *Geochemistry Geophysics Geosystems*, 4, 1073. (doi: 10.1029/2002GC000433)
- Köhler, P., Knorr, G., Buiron, D., Lourantou, A., & Chappellaz, J. (2011). Abrupt rise in atmospheric CO₂ at the onset of the Bolling/Allerod: in-situ ice core data versus true atmospheric signals. *Climate of the Past*, 7, 473-486. (doi: 10.5194/cp-7-473-2011)
- Lambeck, K., & Chappel, J. (2001). Sea level change through the last glacial cycles. *Science*, 292, 679-686. (doi: 10.1126/science.1059549)
- Lambeck, K., Rouby, H., Purcell, A., Sun, Y., & Sambridge, M. (2014). Sea level and global ice volumes from the Last Glacial Maximum to the Holocene. *Proceedings of the National Academy of Sciences*, 111, 15296-15303. (doi: 10.1073/pnas.141176211)
- Lund, D. C., & Asimow, P. D. (2011). Does sea level influence mid-ocean ridge magmatism on Milankovitch timescales? *Geochemistry Geophysics Geosystems*, 12(Q12009). (doi: 10.1029/2011GC003693)
- MacLennan, J., Jull, M., McKenzie, D., Slater, L., & Gronvöld, K. (2002). The link between volcanism and deglaciation in Iceland. *Geochemistry Geophysics Geosystems*, 3(11, 1062). (doi: 10.1029/2001GC000282)
- McKenzie, D., & O'Nions, R. K. (1991). Partial melt distribution from inversion of rare earth element concentrations. *Journal of Petrology*, 32, 1021-1091.
- Miller, K. J., Zhu, W., Montési, L. G. J., & Gaetani, G. A. (2014). Experimental quantification of permeability of partially molten mantle rock. *Earth and Planetary Science Letters*, 388, 273-282. (doi: 10.1016/j.epsl.2013.12.003)
- Nordahl, H., & Ingólfsson, O. (2015). Collapse of the Icelandic ice sheet controlled by sea level rise? *Arktos*, 1, 1-13. (doi: 10.1007/s41063-015-0020-x)
- Pagli, C., & Sigmundsson, F. (2008). Will present day glacier retreat increase volcanic activity? stress induced by recent glacier retreat and its effect on magmatism at the Vatnajökull ice cap, Iceland. *Geophysical Research Letters*, 35(L09304). (doi: 10.1029/2008GL033510)
- Patton, H., Hubbard, A., Bradwell, T., & Schomackere, A. (2017). The configuration, sensitivity and rapid retreat of the Late Weichselian Icelandic ice sheet. *Earth-Science Reviews*, 166, 223-245. (doi: 10.1016/j.earscirev.2017.02.001)
- Peltier, W. R. (2004). Global glacial isostacy and the surface of the ice-age Earth:

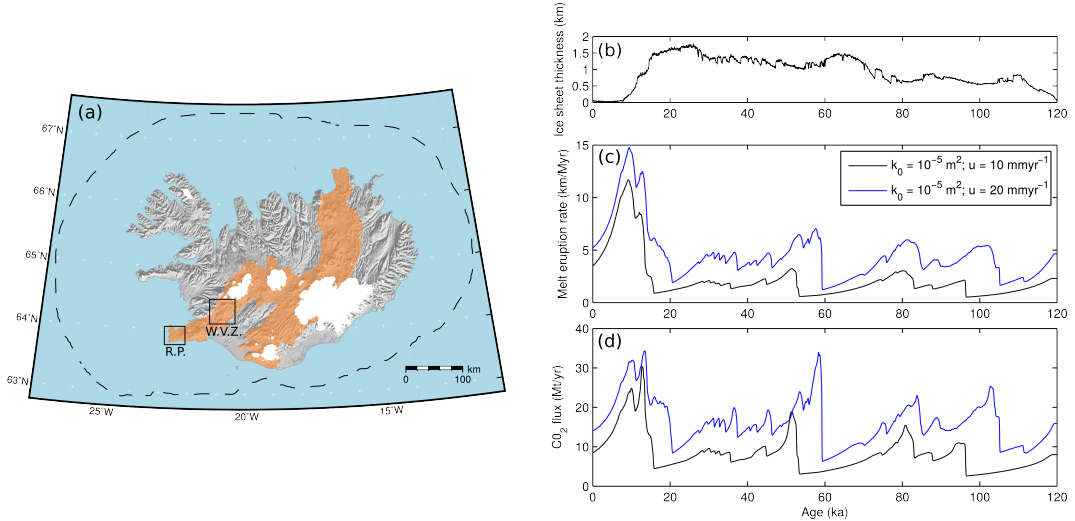
- 371 The ICE-5G (VM2) model and grace. *Annual Reviews of Earth and Planetary*
 372 *Science*, 32, 111-149. (2004)
- 373 Pico, T., Creveling, J. R., & Mitrovica, J. X. (2017). Sea-level records from the
 374 U.S. mid-Atlantic constrain Laurentide Ice Sheet extent during Marine Isotope
 375 Stage 3. *Nature Communications*, 8(15621). (doi: 10.1038/ncomms15612)
- 376 Rawson, H., Pyle, D. M., Mather, T. A., Smith, V. S., Fontjin, K., Lachowcyz,
 377 S. M., & Naranjo, J. A. (2016). The magmatic and eruptive response of arc
 378 volcanoes to deglaciation: Insights from southern Chile. *Geology*, 44, 251-254.
 379 (doi: 10.1130/G37504.1)
- 380 Ribe, N. M. (1985). The generation and composition of partial melts in the earth's
 381 mantle. *Earth and Planetary Science Letters*, 73, 361-376.
- 382 Rosenthal, A., Hauri, E. H., & Hirschmann, M. M. (2015). Experimental determina-
 383 tion of C, F, and H partitioning between mantle minerals and carbonated
 384 basalt, CO₂/Ba and CO₂/Nb systematics of partial melting, and the CO₂
 385 contents of basaltic source regions. *Earth and Planetary Science Letters*, 415,
 386 77-87. (doi: 10.1016/j.epsl.2014.11.044)
- 387 Saal, A. E., Hauri, E. H., Langmuir, C. H., & Perfit, M. R. (2002). Vapour un-
 388 dersaturation in primitive mid-ocean-ridge basalt and the volatile content of
 389 Earths upper mantle. *Nature*, 419, 451-455. (doi: 10.1038/nature01073)
- 390 Schmidt, P., Lund, B., Hieronymus, C., MacLennan, J., Arnadottir, T., & Pagli,
 391 C. (2013). Effects of present-day deglaciation in Iceland on mantle melt
 392 production rates. *Journal of Geophysical Research*, 118, 3366-3379. (doi:
 393 10.1002/jgrb.50273)
- 394 Scott, D. R. (1992). Small-scale convection and mantle melting beneath mid-ocean
 395 ridges. In J. Phipps Morgan, D. K. Blackman, & J. M. Sinton (Eds.), *Mantle*
 396 *flow and melt generation at mid-ocean ridges* (Vol. Geophysical Monograph 71,
 397 p. 327-352). American Geophysical Union.
- 398 Shorttle, O., & MacLennan, J. (2011). Compositional trends of icelandic
 399 basalts: Implications for short-length scale lithological heterogeneity in
 400 mantle plumes. *Geochemistry Geophysics Geosystems*, 12, Q11008. (doi:
 401 10.1029/2011GC003748)
- 402 Sigvaldsson, G. E., Annertz, K., & Nilsson, M. (1992). Effect of glacier load-
 403 ing/delowering on volcanism: postglacial volcanic production rate of the Dyn-
 404 gjufjöll area, central Iceland. *Bulletin of Volcanology*, 54, 385-392. (doi:
 405 10.1007/BF00312320)
- 406 Silbeck, J. N. (1975). On the fluid dynamics of ridge crests. In *Notes on the 1975*
 407 *summer study program in geophysical fluid dynamics at the Woods Hole Oceanographic*
 408 *Institution*, (Vol. 2, p. 113-122).
- 409 Sinton, J., Grönvold, K., & Saemundsson, K. (2005). Postglacial eruptive history
 410 of the Western Volcanic Zone, Iceland. *Geochemistry Geophysics Geosystems*,
 411 6(Q12006). (doi: 10.1029/2005GC001021)
- 412 Sleep, N. H., & Snell, N. S. (1976). Thermal contraction and flexure of mid-
 413 continent and Atlantic marginal basins. *Geophysical Journal of the Royal*
 414 *Astronomical Society*, 45, 125-154.
- 415 Spiegelman, M. (1996). Geochemical consequences of melt transport in 2-D: The
 416 sensitivity of trace elements to mantle dynamics. *Earth and Planetary Science*
 417 *Letters*, 139, 115-132.
- 418 Spratt, R. M., & Lisiecki, L. E. (2016). A late Pleistocene sea level stack. *Climate of*
 419 *the Past*, 12, 1079-1092. (doi: 10.5194/cp-12-1079-2016)
- 420 Sternai, P., Caricchi, L., Castelltort, S., & Champagnac, J. D. (2016). Deglacia-
 421 tion and glacial erosion: A joint control on magma productivity by con-
 422 tinental unloading. *Geophysical Research Letters*, 43, 1632-1641. (doi:
 423 10.1002/2015GL067285)
- 424 Wasylenski, L. E., Baker, M. B., Kent, A. J. R., & Stopler, E. M. (2003). Near-
 425 solidus melting of the shallow upper mantle: partial melting experiments on

426

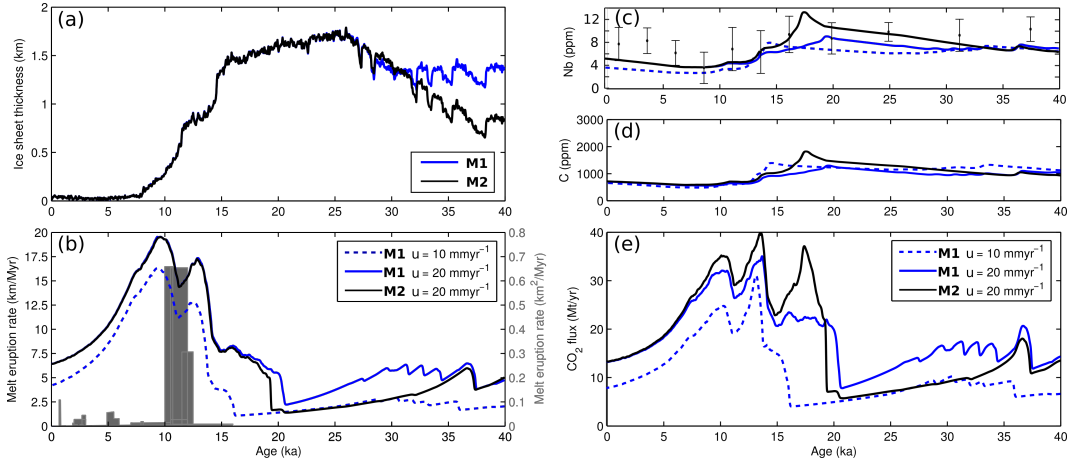
depleted peridotite. *Journal of Petrology*, 44, 116-1191.



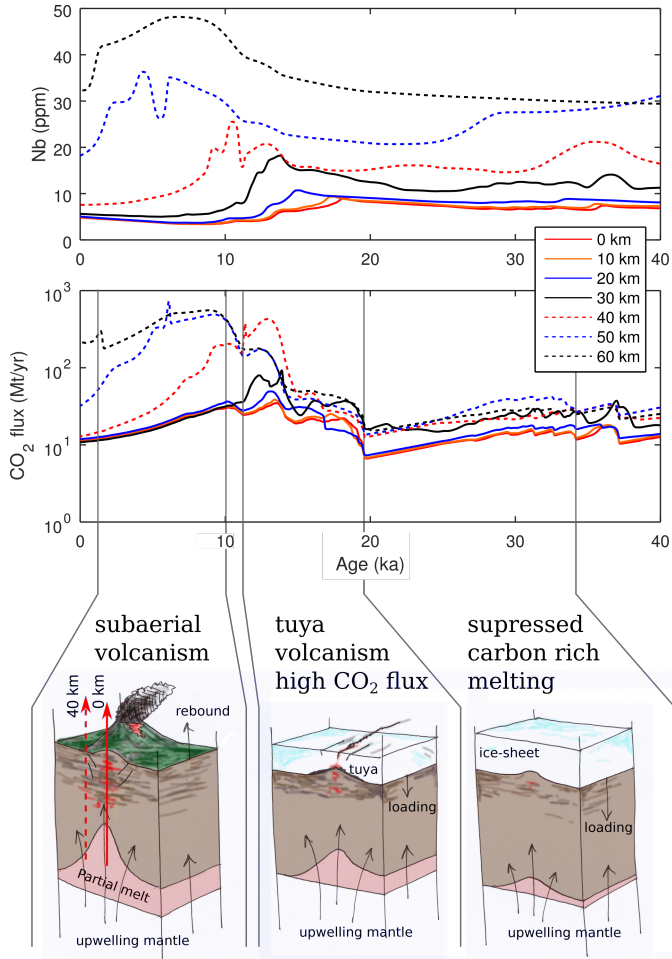
427 **Figure 1.** Profiles of porosity and S-wave seismic velocity for the two model permeabilities of
 428 $k_0 = 10^{-7} \text{ m}^2$ black line, and $k_0 = 10^{-5} \text{ m}^2$ red line. (a) Porosity plotted against depth at steady
 429 state. (b) S-wave velocity from the joint inversion of teleseismic and ambient noise Rayleigh
 430 waves (Harmon & Rychert, 2016) and the predicted S-wave profile from the high permeability
 431 case. The model includes the addition of the adiabatic gradient, the anharmonic effects from the
 432 mineralogy and effects of attenuation (Goes et al., 2012). The dashed line assumes melt has no
 433 effect, the solid line includes a 7.9 % reduction in V_S per percent melt (Hammond & Humphreys,
 434 2000). (c) S-wave velocity predictions for the low permeability case.



435 **Figure 2.** Response of the model to periodic and observed ice sheet thickness changes of the
 436 last 120 ka. (a) Map of Iceland showing the locations of the volcanic rift zones in orange and the
 437 maximum extent of the ice sheet at the last glacial maximum (dashed line). The boxes show the
 438 location of the Reykjanes Peninsular (R. P.) and the Western Volcanic Zone (W. V. Z.). (b) The
 439 ice sheet thickness predicted from the ice sheet model M1 over the last 120 ka. (c) Melt eruption
 440 rate and (d) carbon flux response to the step change in ice sheet thickness: black line, an upper
 441 mantle permeability coefficient of $k_0 = 10^{-5} \text{ m}^2$ and upwelling velocity of 10 mm yr^{-1} , and blue
 442 line, an upwelling velocity of 20 mm yr^{-1} .



443 **Figure 3.** Impact of ice sheet growth and decay on melt eruption and composition over the
 444 last 40 ka. (a) Ice sheet models M1 and M2 taken from the sea-level models of Peltier (2004) and
 445 Pico et al. (2017) respectively. (b) Melt eruption rates (in km of melt per Myr): blue solid line,
 446 ice sheet history M1 for $k_0 = 10^{-5} \text{ m}^2$ with an upwelling rate of 20 mm yr^{-1} ; blue dashed line,
 447 M1 for $k_0 = 10^{-5} \text{ m}^2$ with an upwelling rate of 10 mm yr^{-1} ; black solid line, ice sheet history
 448 M2 for $k_0 = 10^{-5} \text{ m}^2$ with an upwelling rate of 20 mm yr^{-1} . The gray region shows estimated
 449 eruption rates from geological observations [MacLennan et al., 2002] (in km^2 of melt per Myr).
 450 (c) Observed and predicted Nb concentrations (ppm), observations are from the Reykjanes Penin-
 451 sula and the Western Volcanic Zone (Eason et al., 2015; Gee et al., 1998; Sinton et al., 2005),
 452 which are binned at 2.5 kyr intervals from 0 to 17.5 ka and then at 5 kyr intervals. (d) Predicted
 453 variation of in the concentration of carbon (ppm) within the erupted melt. (e) Predicted varia-
 454 tion in the flux of CO₂, assuming that the flux of CO₂ that Icelandic volcanism covers an area of
 455 30,000 km^2 , and CO₂ (ppm) = 3.67 C (ppm) (see Eq. 23 in the Supplementary Material).



456 **Figure 4.** Impact of glacial history on off-axis and on-axis melting. A series of 1D column
 457 melting models forced by the response to deglaciation (ice sheet history model M1) where the
 458 mantle flow is of steady state corner flow. (a) Nb concentrations from the centre of extension out
 459 to 60 km from the centre of extension. The mean concentration weighted by the eruption rate is
 460 plotted as the thick black line. (b) Predicted CO_2 flux from the series of vertical melting models.
 461 The late-Pleistocene eruptions are typified by tuya magmatism. This will have been the case up
 462 until at least ~ 14 ka, where either magmatism was suppressed or when eruptions occurred they
 463 will have been beneath at least 1 km of ice-cover (Hartley et al., 2016). The suppressed melting
 464 regime will have become carbon rich because the shallow low-C melt production is damped due
 465 to the ice-sheet loading. Upon deglaciation there is increased volcanism, which initially taps the
 466 melt rich carbon.